

Leveraging Auxiliary Task Relevance for Enhanced Industrial Fault Diagnosis through Curriculum Meta-learning

Jinze Wang, Tiehua Zhang[†], *Member, IEEE*, Boon Xian Chai, Adriano Di Pietro, Dimitrios Georgakopoulos, *Senior Member, IEEE*, Jiong Jin[†], *Senior Member, IEEE*

Abstract—The accurate diagnosis of machine breakdowns is crucial for maintaining operational safety in smart manufacturing. Despite the promise shown by deep learning in automating fault identification, the scarcity of labeled training data, particularly for equipment failure instances, poses a significant challenge. This limitation hampers the development of robust classification models. Existing methods like model-agnostic meta-learning (MAML) do not adequately address variable working conditions, affecting knowledge transfer. To address these challenges, a Related Task Aware Curriculum Meta-learning (RT-ACM) enhanced fault diagnosis framework is proposed in this paper, inspired by human cognitive learning processes. RT-ACM improves training by considering the relevance of auxiliary working conditions, adhering to the principle of “paying more attention to more relevant knowledge”, and focusing on “easier first, harder later” curriculum sampling. This approach aids the meta-learner in achieving a superior convergence state. Extensive experiments on two real-world datasets demonstrate the superiority of RT-ACM framework.

Index Terms—Fault diagnosis, meta-learning, few-shot, curriculum, task relevance.

I. INTRODUCTION

FAULT diagnosis is crucial for ensuring the safe and efficient operation of machines [1]. Recently, methods based on deep learning (DL) have demonstrated considerable promise in accurately diagnosing machine faults [2]. An advanced ensemble convolutional neural network (CNN) has been introduced for this purpose, utilizing diverse local minima to enhance model adaptability [3]. Furthermore, a capsule network that builds upon CNNs has been proposed for fault classification in bearings [4]. This network combines an inception block and a regression branch, thereby increasing the model’s versatility. However, a notable challenge faced by DL methods is the requirement for extensive training data. Accumulating such data in real-world scenarios is often not feasible due to associated costs and logistical challenges [5].

Jinze Wang, Boon Xian Chai, Adriano Di Pietro are with AIRHUB, Swinburne University of Technology, Melbourne, Australia (email: {jinzewang, bchai, adipietro}@swin.edu.au).

Tiehua Zhang is with the Department of Computer Science and Technology, Tongji University, Shanghai, China (e-mail:tiehuaz@tongji.edu.cn).

Dimitrios Georgakopoulos, Jiong Jin are with the School of Science, Computing and Engineering Technologies, Swinburne University of Technology, Melbourne, Australia (email: {dgeorgakopoulos, jiongjin}@swin.edu.au).

[†] Corresponding author: Tiehua Zhang (tiehuaz@tongji.edu.cn), Jiong Jin (jiongjin@swin.edu.au).

When machines exhibit faults, they are typically partially (e.g., showed down) or fully (e.g., turned off) deactivated for safety reasons, resulting in a scarcity and variety of fault data [6]. Although intentional fault inductions on lab-based machines might provide data, such interventions in operational settings are strictly prohibited. This situation intensifies the challenge of developing reliable DL classifiers for fault diagnosis in real-world contexts [7].

Three key strategies have emerged to tackle the challenge of data scarcity in creating reliable fault diagnosis models: Data Augmentation (DA) [8], Transfer Learning (TL) [9], and Few-Shot Learning (FSL) approaches [10]. At its essence, DA aims to expand and diversify datasets by producing additional data from the limited original samples available. For example, data enhancement techniques that incorporate Gaussian noise, masking noise, and signal translation have been explored in [8]. Moreover, generative models, including variational autoencoders and generative adversarial networks, have been employed to generate fault data for training DL-based diagnostic models in [11]. However, a notable limitation of DA is the potential degradation in data quality and precision, especially when original datasets are sparse. This might reduce the effectiveness of models trained on such data.

To circumvent the limitations of DA, the use of prior knowledge from related tasks has been explored, leading to the concept of Transfer Learning (TL). TL methods strive to utilize knowledge derived from one task to benefit a different, albeit related, task. For instance, a comprehensive one-dimensional CNN architecture, supplemented with fine-tuning mechanisms specifically for fault diagnosis, has been presented [1]. Similarly, a CNN-based model for diagnosing faults in bearings has been proposed, with its basis being knowledge garnered from laboratory bearings data [12]. However, a potential drawback of TL techniques is their inherent emphasis on adapting models to target tasks, which may hinder their broad applicability, especially in environments with limited data [13]. Due to this constraint, there exists a growing need to enhance the overall generalization capabilities of TL methods for more effective fault diagnosis in situations characterized by data sparsity.

Few-shot learning (FSL) stands out for its capability to generalize across tasks, not merely adapting to one. It achieves this by leveraging insights from various auxiliary tasks, a method commonly known as meta-learning [14]. This stands in contrast to transfer learning, where the primary focus is

adaptation to a distinct task. FSL delves deeper by leveraging insights from associated tasks to benefit the primary FSL task [15]. In practical settings, machines typically operate under varied conditions. Gathering substantial data for each specific condition is both expensive and, in some cases, impractical. Yet, when data from varied operational conditions are utilized, a multitude of auxiliary tasks can be formulated. This inherent flexibility renders meta-learning especially fitting and potent for few-shot fault diagnosis scenarios. Such FSL models specifically designed for fault diagnosis have been proposed in [16]. These models frequently incorporate metric-based meta-learning methods, with Siamese neural networks and matching networks being prominent examples.

Despite the potential of metric-based meta-learning methods for feature extraction, their efficacy is hindered by data sparsity and variations in auxiliary task distributions. Model-Agnostic Meta-Learning (MAML) [17], a optimization-based meta-learning method, diverges from traditional metric-based approaches by emphasizing the development of models with robust generalization capabilities. MAML aims to find an initial parameters set, then the model could achieve optimal performance on a series of new tasks after one or more gradient updates, which are calculated using a small amount of data from the series of tasks. Through minimal fine-tuning with target task data, MAML demonstrates superior classification performance in few-shot bearing fault diagnosis. Zhang et al. [18] proposed a MAML-based few-shot learning framework for bearing fault diagnosis with limited data. They achieved this by developing a fault diagnosis model using an improved meta-relation network. Zhou et al. [19] introduced an augmented method that integrates prior knowledge into MAML to fully utilize the prior knowledge present in both training and testing sets. Chen et al. [10] proposed a MAML based model featuring a four-layer CNN capable of feature extraction and rapid adaptation, enabling it to quickly adapt to fault diagnosis tasks under various working conditions. Although these studies have achieved some performance improvements and emphasized that MAML learns to learn, they have overlooked the difficulty level of each task and have not considered the human learning experience of easy-to-hard curriculum learning. Chen et al. [20] propose a novel curriculum hardness aware meta-Learning framework, which incorporates hard sample mining and curriculum learning into a meta-learning paradigm. Hu et al. [6] utilized a specialized task-sequencing strategy for few-shot fault diagnosis, introducing a method where auxiliary tasks are arranged from simple to complex to improve knowledge adaptability during meta-learning. Nevertheless, these existing studies have not considered the relevance between different tasks and the target task. Irrelevant auxiliary tasks may negatively impact the target task.

To simultaneously consider the human easy-to-hard curriculum learning processing and the relevance between different tasks and the target task, we propose a novel Related Task Aware Curriculum Meta-learning (RT-ACM) enhanced fault diagnosis framework, which delicately considers the relevance of patterns among different tasks within the meta-learning paradigm to alleviate data sparsity and task diversity issues. To

begin with, RT-ACM extends MAML to facilitate knowledge transfer to the target task under conditions of limited data. With fault diagnosis in different working conditions treated as single tasks, the initial model weights are meta-learned for faster adaptation to limited training data in target tasks. Furthermore, we design two components in the meta-training process: related task-aware meta-learning and a curriculum strategy to explicitly address the task diversity issue.

Firstly, we exploit the heuristic idea of “pay more attention to more relevant knowledge” to enhance the meta-learner by considering the relevance of auxiliary tasks as related task-aware meta-learning [21]. This approach compels the model to learn more from a combination of tasks that are more similar and are expected to be highly diverse, thereby contributing more to generalization. Specifically, we divide each meta-training round into two stages. In each stage, we first update the meta-learner in a MAML-like manner and then conditionally re-sample a new batch of tasks, focusing on the most complex working conditions based on validation score. Secondly, we propose drawing upon a curriculum strategy to improve the convergence rate and generalization capacity of the meta-learner given the high diversity among different tasks. The underlying concept is to present training tasks to the meta-learner in an “easier first, harder later” paradigm as determined by a teacher recommender [20], [22]. This aims to guide the meta-learner towards a better state. Specifically, we pre-train a teacher recommender for each auxiliary task, use the best validation score to gauge task difficulty, and utilize this knowledge to design a curriculum for the task sampling pool at each meta-training step.

Overall, our main contributions lie in three folds:

- 1) To the best of our knowledge, it is one of the early studies that examines to what extent knowledge can be transferred from auxiliary tasks to the target task by differentiating the relevance of working conditions.
- 2) A novel Related Task Aware Curriculum Meta-learning (RT-ACM) enhanced fault diagnosis framework is proposed, which leverages both transferred knowledge and the diversity of tasks within the target task to mitigate the issue of data sparsity.
- 3) Extensive experiments have been conducted on two real-world datasets to validate the superiority of RT-ACM against state-of-the-art approaches.

The rest of this article is organized as follows. The proposed method is detailed in Section II. In Section III, the effectiveness of RT-ACM is evaluated with various case studies. Finally, Section IV concludes this article and presents future work.

II. PROPOSED RT-ACM

Assume that A auxiliary tasks are available and denoted by $\{T^\mu\}_{\mu=1}^A$. In each auxiliary task, $T^\mu = \{(x_i^\mu, y_i^\mu)\}_{i=1}^M$, where $x_i^\mu \in \mathcal{R}^{1 \times D}$ is i th sample of the input data. In the field of bearing fault diagnosis, 1-D vibration signal is commonly used as the input data. The vibration signal is segmented using a sliding window to generate samples, and D is the length of

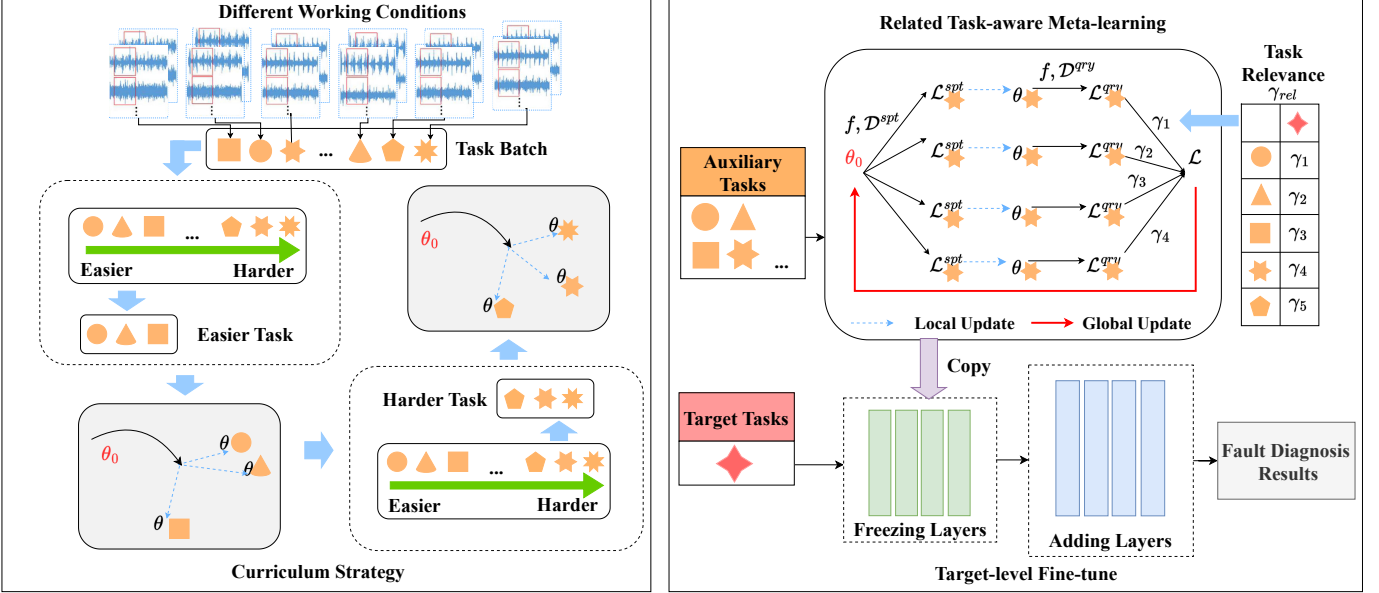


Fig. 1. The overall framework of our proposed RT-ACM.

the sliding window. y_i^μ is the health status of x_i^μ . M denotes the number of samples contained in T^μ .

A target task is denoted by $T^{tar} = \{(x_i^{tar}, y_i^{tar})\}_{i=1}^{M^{tar}}$, where only a few samples are available for training. Thus, M^{tar} , the number of samples contained in T^{tar} , is assigned a very small value. $x_i^{tar} \in \mathcal{R}^{1 \times D}$ is the input data of the i th sample and y_i^{tar} is the corresponding label.

The overview of RT-ACM is outlined in Fig. 1, mainly composed of two channels (i.e., meta-level training on auxiliary tasks and target-level fine-tune). In particular, the meta-level training exploits meta-learning to capture the common vibration pattern by holding the principle of “paying more attention to more relevant knowledge” and learning knowledge curriculum judge by teacher recommender. The goal of target-level fine-tune is to learn the accurate vibration pattern in the target task and performs the predictions.

A. Meta-level Training on Auxiliary Tasks

To distil knowledge from auxiliary tasks and employ vibration patterns, we extend the MAML with long short-term memory (LSTM) [23] as the framework for the meta-learning update. In particular, we devise a related task aware meta-learning and curriculum strategy that can transfer knowledge based on the relevance of patterns among tasks.

1) *Basic Theory of MAML*: Unlike traditional deep learning, as a category of meta-learning, the MAML algorithm is designed to train the initialization parameters of a model within the outer loop. By learning a set of initialization parameters that are sufficiently general, the model can achieve robust performance efficiently with only a few gradient update steps when adapting to new tasks with limited data. From a learning perspective, MAML seeks to identify general internal representations that facilitate transferability to various tasks. Consequently, when confronted with new tasks, only minimal parameter fine-tuning is necessary.

Following [20], the fault diagnosis in different working conditions can be viewed as a single task in a meta-learning paradigm. Thus, the vibration signal of auxiliary tasks $\{T^\mu\}_{\mu=1}^A$ are denoted as $\mathbb{D}_{meta}^{(aux)}$ and the vibration signal of target tasks T^{tar} are divided as training sets $\mathbb{D}_{train}^{(tar)}$ and test sets $\mathbb{D}_{test}^{(tar)}$. We treat each working conditions y_m as a meta-learning task, where each task has support set $\mathcal{D}_{y_m}^{spt}$ for training and a query set $\mathcal{D}_{y_m}^{qry}$ for testing. Finally, our goal is to leverage the auxiliary tasks to learn a meta-learner F_w , which contains knowledge about different working conditions.

Specifically, each iteration of MAML includes local update and global update on the sampled task batch, where the first phase updates θ locally on the $\mathcal{D}_{y_m}^{spt}$ of each task, and the second phase globally updates θ by gradient descent to minimize the sum of loss on the $\mathcal{D}_{y_m}^{qry}$ of all tasks.

- Local update: we first sample a batch of tasks from $\mathbb{D}_{meta}^{(aux)}$. Then we randomly sample a group of vibration signal from $\mathcal{D}_{y_m}^{spt}$ and $\mathcal{D}_{y_m}^{qry}$ for each sampled tasks. Thus, we calculate the training loss on $\mathcal{D}_{y_m}^{spt}$ and locally update θ by one step:

$$\theta'_{y_m} = \theta - \alpha \nabla_{\theta} \mathcal{L}_{y_m}(f_{\theta}, \mathcal{D}_{y_m}^{spt}), \quad (1)$$

where \mathcal{L} is the cross-entropy loss; α is the local learning rate; and θ'_{y_m} is the locally updated recommender parameters on each task.

- Global update: we calculate the testing loss on each $\mathcal{D}_{y_m}^{qry}$ with the corresponding θ'_{y_m} . The MAML global updating aims to update the initialization θ by one gradient step on the sum of all the testing losses:

$$\theta = \theta - \beta \nabla_{\theta} \sum \mathcal{L}_{y_m}(f_{\theta'_{y_m}}, \mathcal{D}_{y_m}^{qry}), \quad (2)$$

where β is the global learning rate.

The optimal parameters of the meta-learning model can be obtained through alternating optimization of the inner and

outer loops. Therefore, the goal of the meta-optimization is to minimize the loss function of the task:

$$\min_{\theta} \sum \mathcal{L}_{y_m}(f_{\theta'_{y_m}}) = \sum \mathcal{L}_{y_m}(f_{\theta} - \alpha \nabla_{\theta} \mathcal{L}_{y_m}(f_{\theta})). \quad (3)$$

2) *Related Task-aware Meta-learning*: Directly transferring patterns from the auxiliary tasks to the target task may introduce noise thus adversely affecting the model performance. By holding the principle of “paying more attention to more relevant knowledge”, we further consider the *relevance of different working conditions* in different tasks when conducting the global update. We obtain the tasks relevance (e.g., γ_{rel}) based on different vibration signal patterns, we thus attentively adapt the gradient across tasks by employing their relevance.

To be specific, we employed autoencoders, a class of unsupervised neural networks, to ascertain the relevance among diverse auxiliary tasks with target task. For three distinct auxiliary tasks as example, represented by datasets \mathcal{Y}_0 , \mathcal{Y}_1 , and \mathcal{Y}_2 , and a target task \mathcal{Y}_{tar} , an autoencoder was trained on their amalgamated data. This model comprises two parts: the encoder f_{enc} and the decoder f_{dec} . In essence, the encoder compresses the input x into a latent representation y , and the decoder attempts to reconstruct x from y . Post-training, the encoder transforms each dataset into this compact latent space, yielding representations μ . For a holistic view of each task, we calculate the mean vector of these representations, denoted as γ_{rel} . The relevance between auxiliary tasks and target task is then quantified using the Euclidean distance:

$$\gamma_{rel_{i,t}} = \frac{1}{\sqrt{1 + \sum_k (\mu_{i,k} - \mu_{t,k})^2}} \quad (4)$$

where indices i designate different auxiliary tasks, t is the target task and k traverses the latent dimensions. The derived distances, namely $\gamma_{rel_{0,t}}$, $\gamma_{rel_{1,t}}$, and $\gamma_{rel_{2,t}}$, serve as task relevance, with values closer to 1 suggesting more related tasks. In other words, if the auxiliary task is more related to the target task, we adapt the gradient so that it updates faster in that direction. There, the Eq.(1) is reformulated as:

$$\theta'_{y_m} = \theta - \alpha \nabla_{\theta} [\mathcal{L}_{y_m}(f_{\theta}, \mathcal{D}_{y_m}^{spt}) \times \gamma_{rel}]. \quad (5)$$

3) *Curriculum Strategy*: In light of the challenges presented by high task diversity, we introduce a novel strategy inspired by the curriculum learning paradigm to enhance the convergence rate and generalization capacity of the meta-learner. We advocate for a sequential presentation of tasks to the meta-learner, adhering to an “easier first, harder later” doctrine. To operationalize this, we introduce a *teacher recommender*. For each auxiliary task, the recommender undergoes preliminary training and uses the highest validation score as an indicator of task difficulty. This metric subsequently informs the design of a curriculum for task sampling at each meta-training iteration. More specific, to quantify the difficulty of a given task, we partition the samples into a training set D_{train} and a validation set D_{valid} . We train a base LSTM model extensively on D_{train} as search recommender. Using the performance metric Φ (e.g., AUC) on the validation set, we ascertain the task-level difficulty, denoted as δ_c . Specifically, δ_c is inversely related to

the highest validation score achieved over all model parameters θ :

$$\delta_c \propto -\max_{\theta} \Phi(f_{\theta}, D_{valid_c} | D_{train_c}) \quad (6)$$

Intuitively, a lower peak validation score indicates more challenging vibration signal pattern within a task.

B. Target-level Fine-tune

After obtaining the general pattern of auxiliary tasks through the meta-learning paradigm, it is important to further fine-tune the learning model for the target task. By investigating the freezing of layers and then fine-tuning, the network generalizes better than one trained directly on the target dataset [24]. This operation not only incorporates information from the auxiliary tasks but also allows for better adaptation to the target task [21].

Specifically, assuming the model (e.g., LSTM) through meta-level training contains L layers, we freeze first l ($1 \leq l \leq L$) layers, while adding n layers after the l layers and fine tune the parameters by using data of the target task, so as to maximize the reusability of the general parameters. Hence, $\mathbf{e}_{hist}^{(tar)}$ is fed into the recurrent layer to infer the hidden state $\mathbf{h}_{t_k}^u$ at t_k , given by,

$$\mathbf{h}_{t_k}^u = LSTM_{frozen}(\mathbf{e}_{hist}^{(tar)}). \quad (7)$$

By doing this, the freezing-layer operation helps generate a network, capable of better balancing the parameters between the auxiliary tasks and target task after the final model fine-tuning.

The probability distribution on all working conditions is calculated by softmax function:

$$\hat{\mathbf{y}} = softmax(f(\mathbf{h}_{t_k}^u)) \quad (8)$$

where f is a fully connected layer to transform $\mathbf{h}_{t_k}^u$ into a $|\mathcal{P}|$ -dimensional vector, and $|\mathcal{P}|$ is the number of faulty class in the target task. Hence, the objective function is defined by:

$$\mathcal{J} = - \sum_{i=1}^{|\mathcal{P}|} \mathbf{y}[i] \cdot \log(\hat{\mathbf{y}}[i]) \quad (9)$$

where \mathbf{y} is an one-hot embedding of the ground-truth fault. Algorithm 1 summarizes the training process of CMEFD, consisting of meta training (lines 3-11), freezing layers and model fine tuning (lines 12-14), as well as fault diagnosis (lines 15-16).

III. CASE STUDY

Rolling bearings play a vital role as essential components in electric machines and find extensive usage across various mechanical equipment. Given the prolonged rotational wear and exposure to high temperatures during operation, bearing failures are common faults that occur. Therefore, conducting research on fault diagnosis in rolling bearings holds significant importance. This study specifically focuses on the detection of faults in rolling bearings within electric motor, considering the varying working conditions and a limited number of available

TABLE I
COMPARISON OF TRADITIONAL DL-BASED AND META-LEARNING-BASED MODELS
(*THE BEST RESULTS ARE HIGHLIGHTED IN BOLD.)

Models	3-way								6-way							
	1-shot				5-shot				1-shot				5-shot			
	T1	T2	T3	T4												
Deep Learning Based																
LSTM	34.65	32.80	37.80	40.75	52.73	42.97	46.46	51.95	20.57	18.32	25.71	27.95	32.86	27.45	30.99	34.67
Cap-Net	41.23	35.56	45.24	47.89	69.53	55.43	65.31	63.74	37.53	31.83	41.02	44.65	63.18	50.29	59.55	57.38
WDCNN	41.50	34.48	45.90	46.07	69.84	55.75	66.93	63.23	37.82	30.92	42.45	44.03	63.68	50.53	60.29	57.05
Meta Learning Based																
MAML	85.23	80.92	83.95	85.80	97.71	95.72	97.03	96.75	70.25	66.38	69.22	71.45	73.59	70.87	72.13	71.68
WCFS	96.77	95.52	97.03	97.70	98.70	97.59	98.88	98.73	85.67	83.32	89.15	87.49	89.68	87.97	93.27	90.15
CHAML	92.95	90.64	93.22	94.86	95.00	93.50	96.21	96.00	88.41	86.61	88.31	90.17	92.67	91.29	90.16	93.61
RT-ACM	98.51	97.44	98.62	98.53	99.68	99.53	99.73	99.56	93.22	92.49	94.38	95.14	97.25	96.59	97.48	97.05

Algorithm 1 Related Task Aware Curriculum Meta-learning (RT-ACM) Enhanced Fault Diagnosis framework

Require: $\mathbb{D}_{meta}^{(aux)}$; learning rates α, β ; number of shots N ;
max step of iterations n ;

- 1: Randomly initialize parameters θ ;
- 2: Calculate the relevance between tasks by Eq.(4);
- 3: Calculate the difficulty of auxiliary tasks by Eq.(6);
- 4: **while** not done **do**
- 5: **for** all $\mathbb{D}_i \in \mathbb{D}_{meta}^{(aux)}$ **do**
- 6: Sample N vibration signal from \mathbb{D}_i as the adapt_batch based on the difficulty;
- 7: Evaluate: $\nabla_{\theta} \mathcal{L}_{y_m}(f_{\theta}, \mathcal{D}_{y_m}^{spt})$ using adapt_batch;
- 8: Calculate the gradient update of θ'_{y_m} by Eq.(5);
- 9: Sample another N vibration signal from \mathbb{D}_i as the eval_batch based on the difficulty;
- 10: **end for**
- 11: Update θ using eval_batch by Eq.(2);
- 12: **end while**
- 13: Freeze the first l layers as new LSTM model, i.e., $LSTM_{frozen}$;
- 14: Fine-tune $LSTM_{frozen}$ using only the target data $\mathbb{D}_{train}^{(tar)}$;
- 15: Predict next possible fault via Eq.(8);
- 16: Calculate the prediction loss for each record via Eq.(9);

samples. To evaluate the effectiveness of the proposed model, a series of case studies are conducted using two widely recognized datasets: the Case Western Reserve University (CWRU) Bearing Dataset [25], the Paderborn University Rolling Bearing Dataset [26] and the Gearbox dataset [19].

Moreover, several state-of-the-art models have been applied for comparison, including LSTM [23], the capsule network (Cap-Net) [4], wide deep CNN (WDCNN) [27], MAML [17], WDCNN-few-shot (WCFS) [10], CHAML [20], PKAML [19]. The LSTM, Cap-Net and WDCNN are DL-based model, MAML, WCFS, CHAML and PKAML are meta-learning based models.

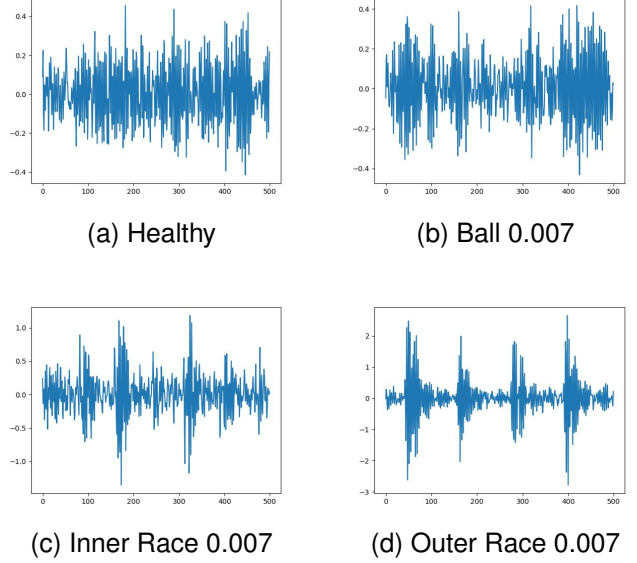


Fig. 2. The visualisation of the vibration signals corresponding to different fault types under same fault diameter and working condition.

A. Case 1: CWRU Bearing Dataset

1) **Dataset Description:** The CWRU dataset has been commonly used to verify DL fault diagnosis methods. The selected rolling CWRU bearing dataset encompasses a comprehensive range of fault types, as depicted in Table II. The dataset comprises four distinct types of electric machine health states, which encompass one normal state and three fault states. The sizes of the faults are specified in terms of diameters, measuring 0.007, 0.014, and 0.021 inches. Fig. 2 provides a visual representation of the vibration signals corresponding to different fault types, all with the same fault diameter. As mentioned in Section II, fault diagnosis under various working conditions can be regarded as different tasks, and each task is a multi-class classification problem. Detailed descriptions of each task and relationship between the motor load and motor speed shown are presented in Table III. We treat one of the tasks as the target task and the rest as auxiliary tasks each time. Following [28], we chronologically divide the dataset of

TABLE II
INFORMATION OF USED BEARINGS FROM CWRU DATASET

Class Label	Fault Type	Fault Diameter (Inches)
1	Healthy	0
2	Ball	0.007
3	Ball	0.014
4	Ball	0.021
5	Inner Race	0.007
6	Inner Race	0.014
7	Inner Race	0.021
8	Outer Race	0.007
9	Outer Race	0.014
10	Outer Race	0.021

TABLE III
DETAILED DESCRIPTIONS OF EACH TASK UNDER CWRU DATASET

Task	Load (hp)	Number of Class	Motor Speed (r/min)
T^1	0	10	1797
T^2	1	10	1772
T^3	2	10	1750
T^4	3	10	1730

the target task into training, validation, and test sets with a ratio of 8:1:1.

2) *Hyper-parameter Settings*: The optimal hyper-parameter settings for all models are empirically found out based on the performance on the validation set. Specifically, for TL-based model, the learning rate is selected from $\{0.1, 0.05, 0.01, 0.005, 0.001, 0.0001\}$, and batch size is set from $\{256, 128, 64\}$. For meta-learning based models, the learning rate α, β are searched from $\{0.1, 0.01, 0.001, 0.0001\}$; and the batch size is set from $\{256, 128, 64\}$ for a fair comparison. For RT-ACM, the number of freezing layers l is searched in range of $[1, 4]$ stepped by one, where the best setting is 3 for all tasks.

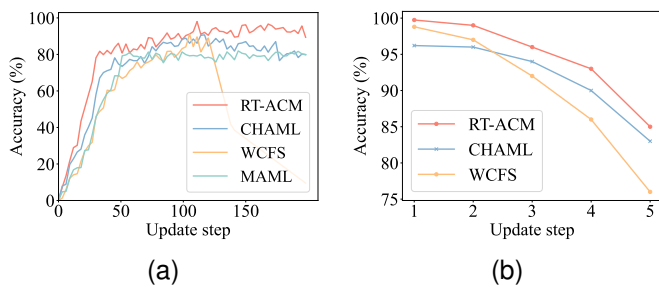


Fig. 3. Accuracy in the (a) outer loop and (b) inner loop.

3) *Performance Comparison*: Table I presents a comprehensive comparison of traditional deep learning-based models and meta-learning-based models across various tasks and shots. The results indicate a clear performance superiority of meta-learning-based models over their traditional counterparts. Specifically, our method RT-ACM consistently achieves the highest accuracy across all scenarios, notably outperforming other models with an impressive accuracy range of 98.51%

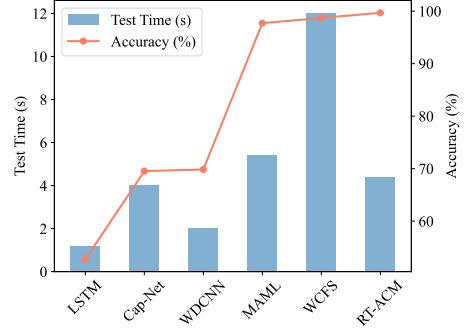


Fig. 4. Model performance on T^1 .

to 99.73% in the 3-way tasks and 93.22% to 97.48% in the 6-way tasks. MAML, WCFS and CHAML, while also meta-learning-based, demonstrate strong performances, especially in the 3-way 5-shot settings. CHAML generally outperforms WCFS due to its structured learning process. By leveraging a curriculum sampling, CHAML progressively exposes the model to increasingly complex tasks, enhancing its ability to generalize and perform well across diverse scenarios. This staged learning process allows the model to build a more robust understanding of the task at hand, resulting in higher accuracy, particularly in more challenging 6-way tasks. Our proposed method RT-ACM integrates related task-aware meta-learning with a curriculum strategy, which further amplifies its performance. The related task-aware mechanism ensures that the model is adept at identifying and leveraging similarities between tasks, thereby improving its efficiency in learning new tasks. Additionally, the curriculum strategy within RT-ACM helps in systematically increasing the difficulty of the tasks presented during training, allowing the model to develop a deeper and more nuanced understanding of the task space. This dual approach not only enhances the learning process but also ensures that the model remains adaptable and highly accurate, as evidenced by its superior performance across all evaluated metrics.

Fig. 3a shows the performance comparison of four meta-learning-based models, in terms of accuracy over increasing global update steps. Our proposed method, RT-ACM, which leverages related task-aware meta-learning and a curriculum strategy, demonstrates a superior ability to rapidly achieve high accuracy. This rapid improvement can be attributed to the efficient transfer of knowledge from related tasks and a structured learning process that progresses from simpler to more complex tasks. In contrast, CHAML, which employs curriculum sampling, lags behind RT-ACM and fails to match its performance throughout the training process due to a less effective related task prioritization. WCFS initially shows competitive accuracy but experiences a decline in performance in later stages, possibly due to overfitting or poor generalization. MAML, while maintaining steady progress, does not achieve the same level of accuracy as RT-ACM. Fig. 3b illustrates the relationship between the performance of model and the number of local update steps. Through empirical analysis, it is observed that a single-step update is adequate to

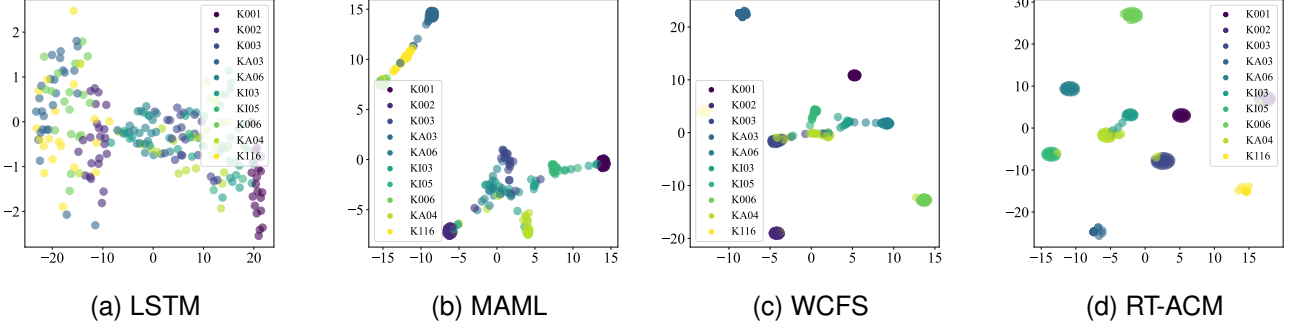


Fig. 5. The visualization of classification from four models.

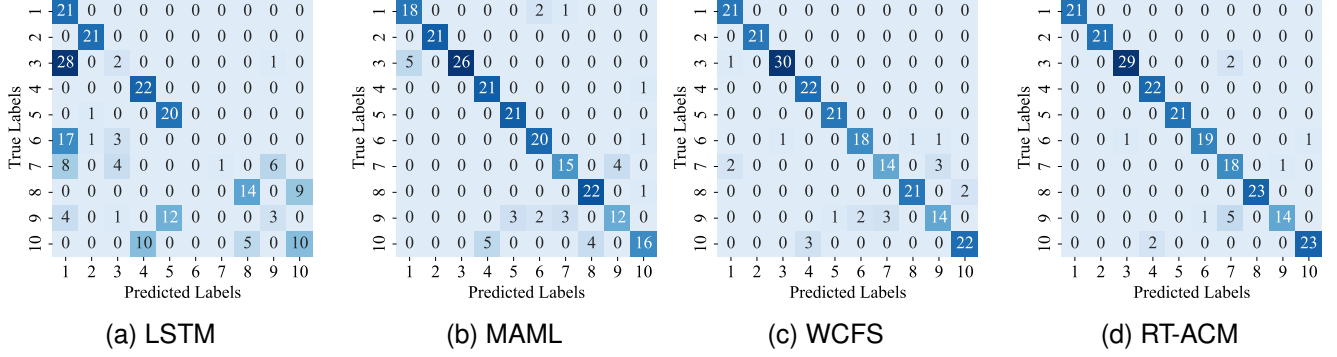


Fig. 6. The visualization of confusion matrices from four models.

enhance the accuracy significantly.

Fig. 4 illustrates that the RT-ACM model stands out for its exceptional combination of efficiency and accuracy on 3-way 5-shot. When compared to conventional models like LSTM and WDCNN, RT-ACM's testing time is considerably shorter, which reflecting its higher processing speed. Additionally, RT-ACM competes closely in accuracy with more sophisticated models like MAML and WCFS. These results highlight the potential of RT-ACM, underscoring the advantages of incorporating auxiliary tasks to enhance the target task in terms of accuracy. Moreover, the curriculum transfer of knowledge from auxiliary tasks in RT-ACM demonstrates rapid learning capabilities.

B. Case 2: PU Bearing Dataset

1) *Dataset Description:* Different from CWRU dataset, the Paderborn University (PU) Bearing Dataset is a pivotal diagnostic tool for rolling bearings include the artificially damaged data. To mitigate the influence of similar bearings on the dataset, vibration signals were collected from 26 bearings characterized by artificial damage, natural damage, and healthy states. The detailed working conditions are presented in Table IV. Following [19], the first 20 bearings were utilized for training, while the remaining 6 bearings were allocated for testing. Each bearing exhibited four distinct working conditions are presented in Table V, primarily varying in rotational speed, load torque, and radial force.

TABLE IV
INFORMATION OF USED BEARINGS FROM PU DATASET

No.	Bearing Code	Faulty Type	Damage Method
1	K003	Healthy	-
2	K004	Helathy	-
3	K005	Healthy	-
4	K006	Healthy	-
5	KA01	Outer Race	Muliple Damage
6	KA03	Outer Race	Electric Engraver
7	KA05	Outer Race	Electric Engraver
8	KA07	Outer Race	Drilling
9	KA08	Outer Race	Drilling
10	KI01	Inner Race	Muliple Damage
11	KI05	Inner Race	Electric Engraver
12	KI07	Inner Race	Electric Engraver
13	KA15	Outer Race	Plastic Deform
14	KA16	Outer Race	Fatigue
15	KA22	Outer Race	Fatigue
16	KB23	Inner/Outer	Fatigue
17	KB27	Inner/Outer	Plastic Deform
18	KI16	Inner Race	Fatigue
19	KI17	Inner Race	Fatigue
20	KI21	Inner Race	Fatigue
21	K001	Healthy	-
22	K002	Healthy	-
23	KA30	Outer Race	Plastic Deform
24	KB24	Inner/Outer	Fatigue
25	KI14	Inner Race	Fatigue
26	KI18	Inner Race	Fatigue

TABLE V
DETAILED DESCRIPTIONS OF EACH TASK UNDER PU DATASET

Task	Rational speed (rpm)	Load torque (Nm)	Radial force (N)
T^1	1500	0.7	400
T^2	900	0.7	1000
T^3	1500	0.1	1000
T^4	1500	0.7	1000

TABLE VI
THE COMPARATIVE METHODS IN PU DATASET (T^1)
(*THE BEST RESULTS ARE HIGHLIGHTED IN BOLD.)

Models	Accuracy		Precision		F1-score	
	10-way		1-shot		5-shot	
	1-shot	5-shot	1-shot	5-shot	1-shot	5-shot
LSTM	40.15	50.89	39.92	50.05	39.61	49.84
MAML	76.85	85.35	76.71	85.19	76.63	85.12
WCFS	78.52	91.07	78.37	90.92	78.45	91.03
CHAML	78.75	90.20	77.61	91.07	78.58	91.13
PKAML	79.20	92.09	79.13	91.97	79.16	92.01
RT-ACM	81.57	94.34	81.43	94.21	81.46	94.27

2) *Evaluation Metrics*: Given the inclusion of artificially damaged data in the PU dataset, resulting in imbalanced distribution, precision and F1 score offer better insights into model performance. Thus, three established evaluation metrics are employed [6]: *Accuracy*, *F1-Score* and *Precision*. Accuracy quantifies the proportion of correct predictions in the total predictions made. It is given by the formula:

$$\text{Accuracy} = \frac{\text{Number of Correct Predictions}}{\text{Total Number of Predictions}}$$

Accuracy provides a general measure of model performance, especially when the class distributions are balanced. Precision is the fraction of relevant instances among the retrieved instances. In other words, it quantifies the accuracy of positive predictions. It is given by:

$$\text{Precision} = \frac{\text{True Positives}}{\text{True Positives} + \text{False Positives}}$$

Precision provides insight into the reliability of positive predictions made by the model. The F1 score is the harmonic mean of precision and recall. It balances the trade-off between precision and recall and is especially useful when the class distribution is imbalanced. It is computed as:

$$\text{F1 Score} = 2 \times \frac{\text{Precision} \times \text{Recall}}{\text{Precision} + \text{Recall}}$$

Where, precision is the proportion of true positive predictions in the set of positive predictions made. Recall is the proportion of true positive predictions in the set of actual positives.

3) *Performance Comparison*: Table VI shows a performance comparison of various models on the PU dataset in 10-way, 1-shot and 5-shot. Notably, all methods except LSTM are meta-learning based approaches, allowing them to handle data sparsity issues more effectively than LSTM. Among these methods, PKAML employs a pretraining process to integrate prior knowledge, enhancing its performance. CHAML utilizes

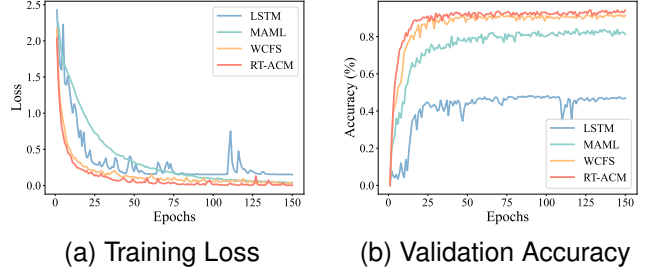


Fig. 7. The visualization of training loss and validation accuracy from four models.

a curriculum sampling in meta-training, providing a structured approach to learning. However, both PKAML and CHAML do not adequately consider the diversity and relevance of auxiliary tasks in relation to the target task, which can limit their effectiveness. In contrast, our proposed method, RT-ACM, incorporates related task-aware meta-learning along with a curriculum strategy, resulting in superior performance. This is evidenced by RT-ACM achieving the highest scores across all metrics and shots, with an accuracy of 81.57% and 94.34% in 1-shot and 5-shot settings, respectively, outperforming the runner-up PKAML and other models significantly.

Fig. 5 presents t-SNE visualizations for four models, highlighting their ability to discriminate between classes. The LSTM visualization shows poorly separated clusters, indicating significant class overlap and lower classification efficacy. MAML improves with tighter clusters but still suffers from overlap at the cluster centers. WCFS slightly betters class separation, with clearer clusters but some outliers. RT-ACM's visualization stands out, with each class forming distinct, isolated clusters, showcasing superior class discrimination and robust classification. The color-coded clusters denote various classes, and RT-ACM's close-knit clusters suggest strong internal similarity and external dissimilarity among classes, reflecting RT-ACM's effective feature space transformation for enhanced class distinction.

Fig. 6 showcases confusion matrices for four classification models, illustrating each model's predictive performance. The LSTM matrix shows widespread misclassifications, such as confusing class 2 with class 3, indicating difficulty in distinguishing similar classes. MAML improves, concentrating predictions along the diagonal but still mixes up classes like 4 and 5. WCFS further enhances accuracy, with clearer diagonal values and fewer errors, notably between classes 7 and 8. RT-ACM stands out with a strong diagonal focus, demonstrating superior accuracy and minimal misclassification, especially distinguishing between closely related classes like 5 and 6, and 9 and 10, where other models struggle. This highlights RT-ACM's robust predictive capability across diverse classes.

Fig. 7a illustrates the training loss of various models, including LSTM, MAML, WCFS, and RT-ACM. The LSTM exhibits significant fluctuations, indicating instability from a small dataset size and potential overfitting issues. In contrast, RT-ACM shows a quick and steady reduction in loss, outperforming MAML and WCFS in terms of learning efficiency and model regularization, suggesting a superior dataset fit.

Fig. 7b compares validation accuracy, with RT-ACM achieving higher accuracy early and maintaining it, highlighting its robustness and generalization capability. LSTM's accuracy fluctuates, while MAML and WCFS improve steadily but don't match RT-ACM's performance. RT-ACM excels in convergence speed and generalization, benefiting from task-aware meta-learning and a curriculum strategy.

IV. CONCLUSION AND FUTURE WORK

In this paper, we develop the Related Task Aware Curriculum Meta-learning (RT-ACM) enhanced fault diagnosis framework, a novel approach in the realm of fault diagnosis for smart manufacturing designed to address the issue of data scarcity. RT-ACM innovatively utilizes auxiliary tasks to enrich the primary fault diagnosis tasks, adhering to the principle of “paying more attention to more relevant knowledge” by focusing on the most relevant knowledge and adopting an “easy-to-hard” curriculum learning strategy. Our comprehensive evaluations across three real-world datasets confirm the effectiveness and superiority of the RT-ACM framework. The experiments not only highlight the efficacy of the framework but also validate the architectural choices, underscoring the potential of combining curriculum strategy with related task aware meta-learning for enhanced fault diagnosis. In future work, we will explore new strategies that can learn both temporal and spatial representations of auxiliary tasks when transferring knowledge to the target task.

REFERENCES

- [1] J. Wu, Z. Zhao, C. Sun, R. Yan, and X. Chen, "Few-shot transfer learning for intelligent fault diagnosis of machine," *Measurement*, vol. 166, pp. 108–202, 2020.
- [2] X. Pang, X. Xue, W. Jiang, and K. Lu, "An investigation into fault diagnosis of planetary gearboxes using a bispectrum convolutional neural network," *IEEE Trans. Mechatron.*, vol. 26, no. 4, pp. 2027–2037, 2020.
- [3] L. Wen, X. Xie, X. Li, and L. Gao, "A new ensemble convolutional neural network with diversity regularization for fault diagnosis," *J. Manuf. Syst.*, vol. 62, pp. 964–971, 2022.
- [4] Z. Zhu, G. Peng, Y. Chen, and H. Gao, "A convolutional neural network based on a capsule network with strong generalization for bearing fault diagnosis," *Neurocomputing*, vol. 323, pp. 62–75, 2019.
- [5] S. Chen, Y. Meng, H. Tang, Y. Tian, N. He, and C. Shao, "Robust deep learning-based diagnosis of mixed faults in rotating machinery," *IEEE Trans. Mechatron.*, vol. 25, no. 5, pp. 2167–2176, 2020.
- [6] Y. Hu, R. Liu, X. Li, D. Chen, and Q. Hu, "Task-sequencing meta learning for intelligent few-shot fault diagnosis with limited data," *IEEE Trans. Ind. Informat.*, vol. 18, no. 6, pp. 3894–3904, 2021.
- [7] Z. Hu and P. Jiang, "An imbalance modified deep neural network with dynamical incremental learning for chemical fault diagnosis," *IEEE Trans. Ind. Electron.*, vol. 66, no. 1, pp. 540–550, 2018.
- [8] X. Li, W. Zhang, Q. Ding, and J.-Q. Sun, "Intelligent rotating machinery fault diagnosis based on deep learning using data augmentation," *J. Intell. Manuf.*, vol. 31, pp. 433–452, 2020.
- [9] F. Zhuang, Z. Qi, K. Duan, D. Xi, Y. Zhu, H. Zhu, H. Xiong, and Q. He, "A comprehensive survey on transfer learning," *Proc IEEE Inst Electr Electron Eng.*, vol. 109, no. 1, pp. 43–76, 2020.
- [10] J. Chen, W. Hu, D. Cao, Z. Zhang, Z. Chen, and F. Blaabjerg, "A meta-learning method for electric machine bearing fault diagnosis under varying working conditions with limited data," *IEEE Trans. Ind. Informat.*, vol. 19, no. 3, pp. 2552–2564, 2022.
- [11] X. Gao, F. Deng, and X. Yue, "Data augmentation in fault diagnosis based on the wasserstein generative adversarial network with gradient penalty," *Neurocomputing*, vol. 396, pp. 487–494, 2020.
- [12] B. Yang, Y. Lei, F. Jia, and S. Xing, "An intelligent fault diagnosis approach based on transfer learning from laboratory bearings to locomotive bearings," *Mech. Syst. Signal Process.*, vol. 122, pp. 692–706, 2019.
- [13] L. Chang and Y.-H. Lin, "Meta-learning with adaptive learning rates for few-shot fault diagnosis," *IEEE Trans. Mechatron.*, vol. 27, no. 6, pp. 5948–5958, 2022.
- [14] D. K. Naik and R. J. Mamonne, "Meta-neural networks that learn by learning," in *IJCNN*, vol. 1. IEEE, 1992, pp. 437–442.
- [15] Y. Wang, Q. Yao, J. T. Kwok, and L. M. Ni, "Generalizing from a few examples: A survey on few-shot learning," *ACM Comput. Surv.*, vol. 53, no. 3, pp. 1–34, 2020.
- [16] J. Long, R. Zhang, Y. Chen, R. Zhao, Z. Yang, Y. Huang, and C. Li, "A customized meta-learning framework for diagnosing new faults from unseen working conditions with few labeled data," *IEEE Trans. Mechatron.*, 2023.
- [17] C. Finn, P. Abbeel, and S. Levine, "Model-agnostic meta-learning for fast adaptation of deep networks," in *ICML*, 2017, pp. 1126–1135.
- [18] S. Zhang, F. Ye, B. Wang, and T. G. Habetsler, "Few-shot bearing fault diagnosis based on model-agnostic meta-learning," *IEEE Trans. Ind. Applicat.*, vol. 57, no. 5, pp. 4754–4764, 2021.
- [19] Y. Zhou, Q. Zhang, T. Huang, and Z. Cai, "Prior knowledge-augmented meta-learning for fine-grained fault diagnosis," *IEEE Transactions on Industrial Informatics*, 2024.
- [20] Y. Chen, X. Wang, M. Fan, J. Huang, S. Yang, and W. Zhu, "Curriculum meta-learning for next poi recommendation," in *SIGKDD*, 2021, pp. 2692–2702.
- [21] J. Wang, L. Zhang, Z. Sun, and Y.-S. Ong, "Meta-learning enhanced next poi recommendation by leveraging check-ins from auxiliary cities," in *PAKDD*. Springer, 2023, pp. 322–334.
- [22] B. X. Chai, B. Eisenbart, M. Nikzad, B. Fox, A. Blythe, P. Blanchard, and J. Dahl, "A novel heuristic optimisation framework for radial injection configuration for the resin transfer moulding process," *Composites Part A: Applied Science and Manufacturing*, vol. 165, p. 107352, 2023.
- [23] S. Hochreiter and J. Schmidhuber, "Long short-term memory," *Neurocomputing*, vol. 9, no. 8, pp. 1735–1780, 1997.
- [24] J. Yosinski *et al.*, "How transferable are features in deep neural networks?" *NeurIPS*, vol. 27, 2014.
- [25] W. A. Smith and R. B. Randall, "Rolling element bearing diagnostics using the case western reserve university data: A benchmark study," *Mech. Syst. Signal Proc.*, vol. 64, pp. 100–131, 2015.
- [26] C. Lessmeier, J. K. Kimotho, D. Zimmer, and W. Sextro, "Condition monitoring of bearing damage in electromechanical drive systems by using motor current signals of electric motors: A benchmark data set for data-driven classification," in *PHM*, vol. 3, no. 1, 2016.
- [27] W. Zhang, G. Peng, C. Li, Y. Chen, and Z. Zhang, "A new deep learning model for fault diagnosis with good anti-noise and domain adaptation ability on raw vibration signals," *Sensors*, vol. 17, no. 2, p. 425, 2017.
- [28] J. Wang, Y. Ren, J. Li, and K. Deng, "The footprint of factorization models and their applications in collaborative filtering," *TOIS*, vol. 40, no. 4, pp. 1–32, 2021.